This article has been accepted for publication in a future issue of this journal, but has not been fully edited. Content may change prior to final publication. Citation information: DOI 10.1109/TCNS.2016.2574129, IEEE Transactions on Control of Network Systems

Efficient Clustering and Path Planning Strategies for Robotic Data Collection Using Space-Filling Curves

Yuan Yan and Yasamin Mostofi

***Abstract*—In this paper, we consider a scenario where a mobile robot is tasked with periodically collecting data from a fixed wireless sensor network. Our goal is to minimize the total cost of the system, including the motion cost of the robot and the communication cost of the sensors to the robot in realistic fading environments. We propose a strategy that divides the sensors into a number of clusters and uses a mobile robot to visit each cluster in order to wirelessly collect the corresponding data. We then propose a computationally-efficient approach to solve this joint path planning and clustering problem by using space-filling curves. More specifically, by utilizing space-filling curves and their locality property, we show how the coupled clustering, stop position selection, path planning and motion design problems can be solved as a series of convex optimization problems. We further mathematically characterize an upper bound for the total energy consumption of our proposed approach for the case of uniformly-distributed sensors, relating it to key motion and communication parameters, such as motor parameters, channel multipath fading and shadowing variances, path loss exponent and target Bit Error Rate (BER). Finally, we verify the effectiveness of our framework in a simulation environment. Our results with realistic channel and motion parameters show a considerable energy saving.**

I. Introduction

In recent years, considerable progress has been made in the area of mobile sensor networks and networked robotic systems [1]–[6]. One application is to use mobile robots (mobile sinks) to harvest data from a wireless sensor network [6]–[10]. In such a scenario, the sensors can be scheduled to transmit information bits to a mobile robot when it gets closer to them, resulting in a smaller communication cost. Along this line, various approaches have been proposed for addressing different issues such as path planning and speed control of the mobile robots [6]–[8]. Visiting each individual sensor, however, can result in long latencies and high motion energy consumption.

In the wireless sensor network literature, clustering is another popular approach for energy saving [11], [12]. In such a framework, the sensors are grouped into a number of clusters with an elected cluster head to manage the data collection in its corresponding cluster. However, each cluster head may need to incur high energy to process and forward the gathered information bits to a remote station.

Naturally, the ideas of clustering and using mobile robots for data collection can be integrated to overcome their individual shortcomings. More specifically, mobile robots can considerably reduce the communication burden of the sensors in each cluster by moving close to the corresponding cluster to collect the data. At the same time, clustering can reduce the motion burden of the robot as it only needs to collect data from one point in the cluster, rather than visiting each sensor individually. Along this line, a number of heuristic approaches have been proposed [13]–[16]. These approaches, however, do not consider realistic fading communication channels. Furthermore, [13]–[15] do not consider motion cost of the robot. [16], on the other hand, considers the motion cost but does not consider trajectory design, assuming fixed trajectories.

Another key aspect of such problems is that communication and motion issues need to be jointly optimized. In general, communication and motion energy co-optimization is an important problem that arises in many robotic network operations that have to operate in realistic environments. In our past work [17]–[20], we considered such co-optimization problems in different contexts. In this paper, we consider a scenario where a mobile robot is tasked with periodically collecting up-to-date data from a wireless sensor network.[1] Our goal is to minimize the total energy cost of the system, including the motion cost of the robot and the communication cost of the sensors to the robot in realistic fading environments. We propose an efficient strategy that jointly optimizes the clustering and path planning of the robot by using space-filling curves. More specifically, the robot first groups the sensors into a number of clusters. A stop position is then optimally chosen in each cluster for the robot to collect the data from the sensors in the corresponding cluster. The robot then periodically visits all the stop positions and gathers the data from the network. We further consider communication over realistic fading links and utilize our previously-proposed probabilistic channel assessment framework to realistically assess the cost of communication [21], [22].

Statement of Contributions: The main challenge of the considered problem is that we need to jointly optimize the number of clusters, the clustering strategy, the stop positions, and the path and motion strategy (motion time/speed along the path) of the robot. As we shall see, this becomes a mixed integer nonlinear program which is difficult to solve. We then propose a computationally-efficient approach to solve this problem by using space-filling curves [23]. We show how the coupled clustering, stop position selection, path planning and motion strategy design problems can be solved sub-optimally but very efficiently as a series of convex optimization problems. Furthermore, we utilize the locality property of space-filling curves to derive an upper bound on the

Yuan Yan and Yasamin Mostofi are with the Department of Electrical and Computer Engineering, University of California, Santa Barbara, USA (email:{yuanyan,ymostofi}@ece.ucsb.edu). This work is supported in part by NSF NeTS award # 1321171.

[1] Our proposed strategy can be extended to the scenario where the robot only needs to collect the data once from the network. In this case, the initial position of the robot should also be taken into account. Characterizing the details of this case is a subject of our future work.

This article has been accepted for publication in a future issue of this journal, but has not been fully edited. Content may change prior to final publication. Citation information: DOI 10.1109/TCNS.2016.2574129, IEEE Transactions on Control of Network Systems

total energy consumption of the operation, relating it to key motion, communication, and system parameters. As compared to the conference version of this work [24], in this paper we consider a more realistic motion model that takes the impact of velocity and acceleration of the robot into account, which requires new derivations and analysis. We further propose an iterative algorithm to jointly optimize the stop positions, the clustering strategy, and the path and motion strategy of the robot. Finally, we extend our approach to the case of non-uniformly-distributed sensors over the environment.

The rest of the paper is organized as follows. Section II describes the motion and communication models, introduces the basic properties and applications of the space-filling curves, and formulates the general optimization problem. Section III presents the first part of our proposed framework for the case where the sensors are uniformly distributed in the workspace and characterizes its performance bound. Section IV presents the second part of our framework, an additional iterative fine-tuning inspired by Lloyd's algorithm. Section V then extends our framework to the case where the sensors are not uniformly distributed. Section VI shows the performance of our proposed framework in a simulation environment with realistic communication and motion parameters. We conclude in Section VII.

II. Problem Setup

Consider a scenario where a robot is tasked with periodically collecting data from a fixed wireless sensor network. The robot does not know the exact positions of the sensors, but only the probability distribution of their positions. More specifically, we assume that a total of m stationary sensors are independent and identically distributed according to a probability density function (pdf) $p(x)$ in a square workspace $\mathcal{W}$ with the side length of D. Each sensor collects the data from the environment with a rate of ρ bits/second and caches it in its memory. A robot is then tasked with gathering the up-to-date data from all the sensors in a given period T. Our goal is to minimize the total energy cost of the whole operation in each period, including the communication energy cost of the sensors and the motion cost of the robot. Clearly, the motion cost is minimized if the robot stays at some point in the workspace while the sensors transmit their gathered bits to it. However, such a strategy is not energy efficient for communication. On the other hand, the communication cost can be minimized if the robot visits each sensor to download the data. However, this strategy causes a high motion cost for the robot.

In this paper, we propose a strategy that properly combines the ideas of clustering and robotic data collection in a wireless sensor network. In such a strategy, all the sensors are divided into a number of clusters. A stop position is chosen in each cluster for the robot to collect the data (via single-hop wireless transmissions) from the sensors in the corresponding cluster. In this paper, we assume that the robot can only collect data when it stops at its stop positions. The robot then periodically visits all the stop positions and gathers the data from the network. Fig. 1 shows an example of our considered scenario. In general, the motion cost can increase as the number of clusters increases since the robot needs to travel a longer distance in each period. On the other hand, the communication cost can decrease as the number of clusters increases, since the transmission distances of the sensors decrease. Hence, in this problem, we need to jointly optimize the number of clusters, the clustering of the network, the stop positions, and the path planning and motion strategy of the robot, in order to minimize the total energy cost.

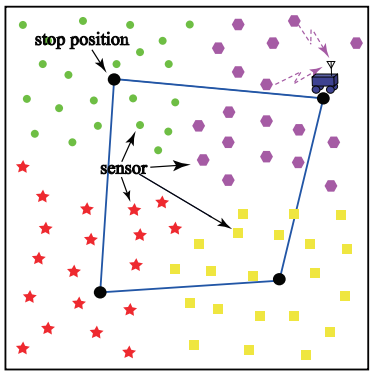

Fig. 1. An example of using a robot to gather the data from a sensor network. The sensors are divided into 4 clusters. Markers with the same color and shape represent the sensors that are clustered together. The robot has to decide on an optimal stop position in each cluster and then visits all the stop positions periodically to wirelessly collect the data from the sensors in the corresponding clusters.

Remark 1: For simplicity, we only consider the case of single-hop transmissions in this paper. Moreover, we assume that the sensors can send their information bits to the robot only when it stops at its stop positions. As a result, the communication cost only depends on the clusters and stop positions, as we shall show later. For the case of multi-hop transmissions, routing strategies in each cluster also need to be jointly designed. If the robot is allowed to collect data while moving, the communication cost will depend on the trajectory of the robot rather than the stop positions. Extension to these two cases is the subject of our future work.

In the rest of this section, we first introduce the concept of space-filling curves which we shall use for algorithm design and performance analysis. We then present the communication and motion models. Finally, we formulate the general optimization problem that we need to solve in this paper.

A. Space-Filling Curves [23], [25]

A space-filling curve is a one-dimensional curve that passes through every point of a two-dimensional square. Some of the most celebrated ones are the Hilbert curve, Peano curve and Sierpiński curve. Readers are referred to [23] for more details on various space-filling curves and how to recursively construct them.

Because of their recursive and self-similar construction, one of the most important properties of space-filling curves is the *locality* property, which means that any two points that are close in the one-dimensional space are mapped to two points that are close in the 2D space. More specifically, let $\mathrm{SF}(\cdot) : \mathcal{C} \rightarrow \mathcal{W}$ denote the continuous mapping of a

This article has been accepted for publication in a future issue of this journal, but has not been fully edited. Content may change prior to final publication. Citation information: DOI 10.1109/TCNS.2016.2574129, IEEE Transactions on Control of Network Systems

space-filling curve from the unit circle to the $[0, D]^2$ square workspace, where $\mathcal{C} = [0, 1)$ represents the unit circle with a fixed reference point at 0. Note that $\phi \in \mathcal{C}$ represents a point on $\mathcal{C}$, clockwise, from the reference point. Then, we have [23], [26]

$$\|x_1 - x_2\| \leq C_{\text{SF}} \times D \times \mu(\phi_1, \phi_2), \tag{1}$$

where $\phi_1, \phi_2 \in \mathcal{C}$, $x_1 = \text{SF}(\phi_1) \in \mathcal{W}$, $x_2 = \text{SF}(\phi_2) \in \mathcal{W}$, C_{SF} is a constant depending on the type of the space-filling curve, $\mu(\phi_1, \phi_2) = \min\{|\phi_1 - \phi_2|, 1 - |\phi_1 - \phi_2|\}^{1/2}$, and $\|\cdot\|$ and $|\cdot|$ denote the Euclidean norm and absolute value of the argument respectively. See Fig. 2 for an illustration of the mapping. For Sierpiński curves, for instance, $C_{\text{SF}} = 2$ [23], [26].[2] Note that $\text{SF}(\cdot)$ is not a one-to-one mapping. Different points in $\mathcal{C}$ can be mapped to the same point in $\mathcal{W}$. See [23], [26], [27] for more details on how $\text{SF}(\cdot)$ and $\text{SF}^{-1}(\cdot)$ are evaluated in practice.

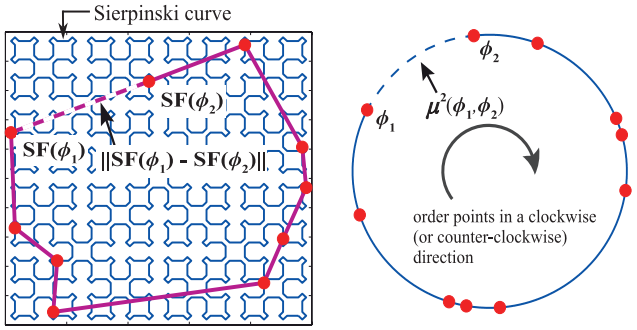

Fig. 2. The blue curve in the left figure shows the construction of the Sierpiński curve after four recursions in the 2D workspace. The right figure then shows the corresponding 1D curve (circle). The red dots in the left and right figures show the positions of the points in the square and their corresponding mapping in the unit circle respectively. The figure then shows an illustration of the mapping $\text{SF}(\cdot)$ and $\mu(\cdot, \cdot)$. The figure also shows how this mapping can be used to solve a TSP problem, where the line segments that connect the points in the square form the tour obtained based on the ordering of the points in the unit circle [25].

Due to this *locality* property, space-filling curves are widely used in computational science [23]. The application that is most related to this paper is to solve the Traveling Salesman Problem (TSP) as follows [26], [27]. First, map all the points in the square into the unit circle using $\text{SF}^{-1}(\cdot)$. Then, order the mapped points on the unit circle in a clockwise or counter-clockwise direction. Finally, build the tour by connecting the corresponding points in the square based on this order. Fig. 2 shows an illustration of solving the TSP problem by using this approach. When the points are independent and identically distributed (i.i.d.) and the number of points are large, the heuristic tour is roughly 35% away from the optimum [27]. However, the computational complexity of this approach is extremely low. In [25], we showed how to utilize the space-filling curves to solve a communication-aware dynamic coverage problem. In this paper, we utilize them for clustering and data collection in a sensor network.

Remark 2: There are a number of efficient heuristic algorithms in the TSP literature that can be potentially used towards solving the considered problem [28], [29]. In this paper, however, we use space-filling curves since they allow us to not only efficiently choose the stop positions and plan the TSP tour but also to characterize the performance bound of our proposed approach.[3]

[2]In this paper, we use Sierpiński curves in our simulations. This is because constant C_{SF} of Sierpiński curves is among the smallest in the space-filling curves family [23]. This then has the potential to improve the performance of heuristic algorithms which take advantage of their locality property.

B. Spectral Efficiency and Communication Energy Model

The communication quality is acceptable if the received Bit Error Rate (BER) at the robot is below a given threshold. Assume that the commonly-used MQAM modulation is used for communication. We then have the following for the minimum required communication power from a sensor at position x to the robot at position q [30]: $\widetilde{P}_{\text{C}}(x, q) = (2^R - 1)/(K\gamma(x, q))$, where $\widetilde{P}_{\text{C}}(x, q)$ denotes the communication power, R represents the spectral efficiency (transmission rate divided by the given bandwidth), $\gamma(x, q)$ is the received Channel-to-Noise Ratio (CNR) in the transmission from the sensor at position x to the robot at position q, $p_{b,\text{th}}$ is the target BER, and $K = -1.5/\ln(5p_{b,\text{th}})$. The total communication energy cost of a sensor in each period can then be characterized as $\widetilde{E}_{\text{C}}(x, q) = \widetilde{P}_{\text{C}}(x, q)\rho T/(BR)$, where B is the available communication bandwidth.[4]

In this paper, we consider realistic channels that experience path loss, shadowing and multipath fading. Then, CNR ($\gamma(x, q)$) can be modeled as a lognormal random variable [21], [22]. For the purpose of planning, the robot needs to predict the channel at unvisited locations. The robot can then use our previously-proposed probabilistic channel prediction framework to predict the CNR at unvisited locations, based on a small number of a priori sample measurements in the same environment [21], [22]. This framework characterizes the distribution of the channel at an unvisited location by conditioning on the available samples. Readers are referred to [21], [22] for more details. In this paper, we consider the case where the channel (shadowing component) is spatially uncorrelated. The channel (in dB) from sensor at position x can then be characterized by a Gaussian random variable with mean $\widetilde{\alpha}_{\text{dB}} - 10n_{\text{PL}}\log_{10}(\|x - q\|)$ and variance σ^2_{dB}, where $\widetilde{\alpha}_{\text{dB}}$ is the path loss parameter, n_{PL} represents the path loss exponent (typically around $2 \sim 6$ [30]), and σ^2_{dB} denotes the variance of the channel (both shadowing and multipath fading). These parameters can be estimated on the field as shown in [21], [22].

Since we are predicting the channel quality probabilistically, the anticipated communication energy cost $\widetilde{E}_{\text{C}}(x, q)$ becomes a random variable as well. We then take its average (over the predicted channel) as our communication cost:

$$E_{\text{C}}(x, q) = \frac{2^R - 1}{K}\mathbb{E}\left\{\frac{1}{\gamma(x, q)}\right\}\frac{\rho T}{BR} = P_{\text{C}}(x, q)\frac{\rho T}{BR}. \tag{2}$$

[3]The computational complexity of the approaches proposed in [28] and [29] are $O(N^2)$ and $O(N(\log(N))^{O(c)})$, respectively, where N is the number of TSP stop positions and c is a constant. For comparison, the complexity of the space-filling-based approach [26] is $O(N\log(N))$.

[4]Note that in this paper, we assume that the sensor network uses Time Division Multiple Access such that only one sensor in the network communicates to the robot at a given time slot. Equivalently, we can also use Frequency Division Multiple Access so that the sensors in each cluster simultaneously communicate to the robot.

This article has been accepted for publication in a future issue of this journal, but has not been fully edited. Content may change prior to final publication. Citation information: DOI 10.1109/TCNS.2016.2574129, IEEE Transactions on Control of Network Systems

From [21], [22], we have:

$$\mathbb{E}\left\{\frac{1}{\gamma(x,q)}\right\} = \exp\left(\left(\frac{\ln 10}{10}\right)^2 \frac{\sigma_{\text{dB}}^2}{2}\right) \widetilde{\alpha}\|x-q\|^{n_{\text{PL}}} = \alpha\|x-q\|^{n_{\text{PL}}}, \quad (3)$$

where $\widetilde{\alpha} = 10^{\widetilde{\alpha}_{\text{dB}}/10}$. Hence, the average communication energy cost decreases as the path loss exponent decreases and/or the shadowing/multipath variance decreases. Moreover, for this uncorrelated channel model, it can be seen that it is always optimal for a sensor to transmit its bits to the closest stop position of the robot. However, the cost is different from the case of path-loss-only modeling as channel shadowing and multipath variances are included in α.

C. Motion Energy Model

Consider the case where the robot uses DC motors for its motion. Then, the motion power cost of the robot can be characterized as follows [31]: $P_{\text{M}}(v,a) = \kappa_1 v^2 + \kappa_2 v + \kappa_3 a^2 + \kappa_4 + \kappa_5 a + \kappa_6 av$, where $P_{\text{M}}(v,a)$ is the motion power cost, v and a denote the velocity and acceleration of the robot, respectively, and positive constants κ_i, for $i \in \{1,\cdots,6\}$, are the corresponding motor parameters. Since the initial and final velocities of the robot are both zero when traveling from one stop position to another, we can neglect the last two terms in $P_{\text{M}}(v,a)$ [31].

Then, the motion energy cost for traveling along a trajectory with length d, given a motion time t_{mo}, can be found by solving the following optimal control problem:

$$\begin{aligned} \text{minimize} \quad & \int_0^{t_{\text{mo}}} (\kappa_1 v^2(\tau) + \kappa_2 v(\tau) + \kappa_3 a^2(\tau) + \kappa_4) d\tau \\ \text{subject to} \quad & \dot{q}(t) = v(t), \quad q(0) = 0, \quad q(t_{\text{mo}}) = d, \\ & \dot{v}(t) = a(t), \quad v(0) = 0, \quad v(t_{\text{mo}}) = 0, \end{aligned} \quad (4)$$

where $q(t)$ denotes the position of the robot, $q(0) = 0$ and $q(t_{\text{mo}}) = d$ denote the initial and terminal positions of the robot respectively, and $v(0) = 0$ and $v(t_{\text{mo}}) = 0$ are the initial and terminal velocities of the robot respectively. Here, the control input we need to optimize is $a(t)$. Note that for a fixed t_{mo}, equation (4) can be solved analytically by using optimal control theory [32]. After several steps of calculations, it can be shown that the optimal motion cost is as follows:

$$E_{\text{mo}}(d, t_{\text{mo}}) = \frac{\kappa_1 d^2}{t_{\text{mo}} - 2\sqrt{\frac{\kappa_3}{\kappa_1}} \frac{\exp\left(\sqrt{\kappa_1/\kappa_3} t_{\text{mo}}\right) - 1}{\exp\left(\sqrt{\kappa_1/\kappa_3} t_{\text{mo}}\right) + 1}} + \kappa_2 d + \kappa_4 t_{\text{mo}}. \quad (5)$$

Note that $\lim_{t_{\text{mo}} \to 0} E_{\text{mo}}(d, t_{\text{mo}}) = \infty$ if $d > 0$. For convenience, we then define $E_{\text{mo}}(d, t_{\text{mo}}) = \infty$ for the case where $t_{\text{mo}} = 0$ and $d > 0$. Also, we define $E_{\text{mo}}(d, t_{\text{mo}}) = 0$ for the case where $t_{\text{mo}} = 0$ and $d = 0$.

The following lemma shows the convexity of $E_{\text{mo}}(d, t_{\text{mo}})$ with respect to t_{mo}, which will be used in later sections.

Lemma 1: $E_{\text{mo}}(d, t_{\text{mo}})$ is a convex function of t_{mo} for $t_{\text{mo}} \in (0, \infty)$.

Proof: The lemma can be verified by characterizing the second-order derivative of $E_{\text{mo}}(d, t_{\text{mo}})$. ■

D. Optimization Framework

In this part, we formulate the general optimization problem that we need to solve based on the previously-discussed communication and motion models.

Consider the case where the robot divides the sensors into N clusters. Note that N is an unknown variable. Let $\{\mathcal{W}_i\}_{i=1}^N$ denote a partition of the workspace such that the sensors in $\mathcal{W}_i$ form a cluster. Also, let q_i, for $i \in \{1,\cdots,N\}$, represent the stop position to collect data from the sensors in the i^{th} cluster. Then, based on the communication model in Section II-B, the total average communication cost of the sensors can be characterized as follows:

$$E_{\text{tot,comm}}(N, \mathcal{Q}, \{\mathcal{W}_i\}_{i=1}^N) = m \sum_{i=1}^N \int_{\mathcal{W}_i} p(x) P_{\text{C}}(x, q_i) \frac{\rho T}{BR} dx,$$

where $\mathcal{Q} = \{q_1, \cdots, q_N\}$ denotes the set of stop positions. Therefore, we have the following optimization problem to minimize the total energy cost of the network:

$$\begin{aligned} \text{min.} \quad & E_{\text{tot}}(N, \mathcal{Q}, \{\mathcal{W}_i\}_{i=1}^N, \{t_{\text{mo},i,j}\}_{i,j=1}^N, \mathcal{T}) = \\ & \underbrace{m \sum_{i=1}^N \int_{\mathcal{W}_i} p(x) P_{\text{C}}(x, q_i) \frac{\rho T}{BR} dx}_{E_{\text{tot,comm}}(N, \mathcal{Q}, \{\mathcal{W}_i\}_{i=1}^N)} \\ & + \underbrace{\varpi \sum_{i=1}^N \sum_{j=1, j\neq i}^N z_{i,j} E_{\text{mo}}(\|q_i - q_j\|, t_{\text{mo},i,j})}_{E_{\text{tot,mo}}(N, \mathcal{Q}, \{t_{\text{mo},i,j}\}_{i,j=1}^N, \mathcal{T})} \end{aligned} \quad (6)$$

$$\begin{aligned} \text{s.t.} \quad & 1) \sum_{i=1, i\neq j}^N z_{i,j} = 1, \forall\, j, \quad 2) \sum_{j=1, j\neq i}^N z_{i,j} = 1, \forall\, i, \\ & 3) \, u_i - u_j + (N-1) z_{i,j} \leq N - 2, \forall\, i, j \neq 1, i \neq j, \\ & 4) \sum_{i=1}^N \sum_{j=1, j\neq i}^N z_{i,j} t_{\text{mo},i,j} \leq T\left(1 - \frac{m\rho}{BR}\right), \\ & 5) \, t_{\text{mo},i,j} \geq 0, \forall\, i, j, \quad 6) \, z_{i,j} \in \{0,1\}, \forall\, i, j, \\ & 7) \, u_i \in \{2, \cdots, N\}, \forall\, i \neq 1, \quad 8) \, q_i \in \mathcal{W}, \forall\, i, \end{aligned}$$

where $E_{\text{tot}}(N, \mathcal{Q}, \{\mathcal{W}_i\}_{i=1}^N, \{t_{\text{mo},i,j}\}_{i,j=1}^N, \mathcal{T})$ and $E_{\text{tot,mo}}(N, \mathcal{Q}, \{t_{\text{mo},i,j}\}_{i,j=1}^N, \mathcal{T})$ represent the total cost of the network and the total motion energy cost, respectively, $\varpi > 0$ is a weight balancing the importance of the average communication energy cost of the sensors and the motion energy cost of the robot, $\mathcal{T}$ is the tour of the robot to visit the stop positions, $t_{\text{mo},i,j}$ is the motion time moving from q_i to q_j, $z_{i,j}$ denotes a binary variable which is 1 if the tour of the robot contains the line segment from q_i and q_j and is 0 otherwise, and u_i is an auxiliary integer variable, which designs the tour.

The first and second constraints in (6) guarantee that each stop position has one degree out and one degree in, respectively. The third constraint is the Miller-Tucker-Zemlin (MTZ) sub-tour elimination constraint [33]. Hence, constraints 1-3 ensure that the solution will form a Hamiltonian cycle. The

This article has been accepted for publication in a future issue of this journal, but has not been fully edited. Content may change prior to final publication. Citation information: DOI 10.1109/TCNS.2016.2574129, IEEE Transactions on Control of Network Systems

fourth constraint guarantees that the sum of the total motion and communication times is less than or equal to the total time budget.

The variables to solve for are N, q_i, $\mathcal{W}_i$, $t_{\text{mo},i,j}$, $z_{i,j}$ and u_i. Note that we assume $BR \geq m\rho$ such that the problem is feasible. It is straightforward to see that if the equality holds, the optimal solution is that the robot stays at some position in the workspace to collect the data without moving. Also, without loss of generality, we only consider the case where the robot travels along the line segments between the stop positions, since the motion cost is monotonically increasing with respect to the travel distance between any two stop positions, as can be seen in (5). Hence, the tour $\mathcal{T}$ is completely determined by variable $z_{i,j}$, i.e. the order in which to visit the stop positions.

As can be seen, the optimization problem (6) is a mixed integer nonlinear program. Moreover, all the variables are coupled. For instance, N and $\mathcal{Q}$ affect not only the communication cost of the sensors (since each sensor transmits to its closest stop position), but also the motion cost of the robot. However, even for fixed N, $\mathcal{Q}$ and $\{\mathcal{W}_i\}_{i=1}^N$, jointly determining the tour and the corresponding motion times, i.e. solving $z_{i,j}$ and $t_{\text{mo},i,j}$, is still NP-hard.

In the rest of the paper, we then show how to sub-optimally but efficiently solve (6). More specifically, we first determine the number of clusters and design an initial solution by taking advantage of the locality property of the space-filling curves (Algorithm 1 for the case of uniformly-distributed sensors and Algorithm 3 for the case of non-uniformly-distributed sensors, as we shall discuss in Sections III and V respectively). Then, we propose an iterative approach (Algorithm 2) to optimize the stop positions, the clustering strategy, and the path and motion strategy of the robot after the initial phase. Fig. 3 shows a flow chart of our approach. We shall see how each step of our proposed approach boils down to solving a series of convex optimization problems.

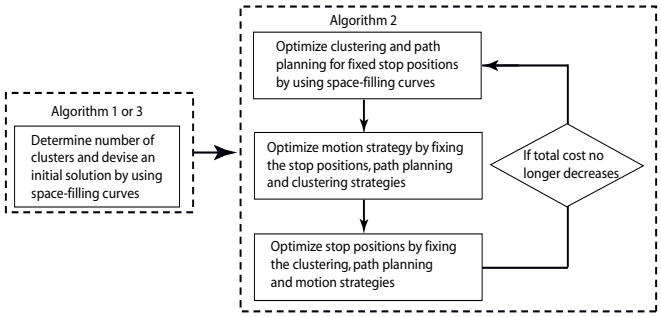

Fig. 3. Flow chart of our proposed approach. We first determine the number of clusters and design an initial solution by using space-filling curves (Algorithm 1 for the case of uniformly-distributed sensors and Algorithm 3 for the case of non-uniformly-distributed sensors). Then, we iteratively optimize the stop positions, the clustering strategy, and the path and motion strategy of the robot (Algorithm 2).

Lemma 2: If the stop positions $\mathcal{Q}$ are given, the optimal solution of $\{\mathcal{W}_i\}_{i=1}^N$ for the case of uncorrelated channels will always be the Voronoi partition $\{\mathcal{V}_i(\mathcal{Q})\}_{i=1}^N$.[5]

Proof: Since the communication cost is monotonically increasing with respect to the distance between a sensor and the robot, the result follows straightforwardly. ■

Lemma 2 implies that the underlying variables to solve for are N, q_i, $t_{\text{mo},i,j}$, $z_{i,j}$ and u_i in (6). We will use Lemma 2 in the subsequent sections when designing our algorithm.

III. Joint Clustering and Path Planning

In this section, we present the initial phase of our proposed approach to solve the optimization problem of (6) based on space-filling curves. We consider uniformly distributed sensors in this part, i.e. $p(x) = 1/D^2$. We show how the initial design can be simplified to solving a series of convex optimization problems. Moreover, we characterize how the number of clusters is related to the communication and motion parameters. Finally, we compare the upper bound of the performance of the proposed approach to the case of no clustering (i.e. the whole workspace is one cluster) to show its benefits. We then extend our results to the case of non-uniformly distributed sensors in Section V.

A. Our Proposed Approach

Consider the case where there is no clustering, i.e. there is only one cluster (the whole workspace). In the rest of the paper, this case will serve as a benchmark for comparison. It can be easily seen that the optimal stop position ($q_1^\star$) is the center of the workspace in this case since the sensors are uniformly distributed.[6] The optimal value of (6) is as follows for $N = 1$:

$$\begin{aligned} E_{\text{tot,noCl,unif}} &= m \int_{\mathcal{W}} \frac{1}{D^2} P_{\text{C}}(x, q_1^\star) \frac{\rho T}{BR} dx \\ &= \frac{m\alpha D^{n_{\text{PL}}}(2^R - 1)\rho T C_1}{KBR}, \end{aligned} \tag{7}$$

where $E_{\text{tot,noCl,unif}}$ denotes the total energy cost for the case of no clustering and $C_1 = \int_{-0.5}^{0.5}\int_{-0.5}^{0.5} \|x\|^{n_{\text{PL}}} dx$.

Note that optimally solving our general optimization problem of (6) is not possible. Instead, we propose the following approach to efficiently decouple the optimization of the stop positions, the tour, and the motion times.

1) Optimization of the stop positions (variables q_is): Since the sensors are uniformly distributed, we expect that in general the stop positions should be evenly located across $\mathcal{W}$, especially when the communication cost is dominant. This design can be easily achieved in the space-filling curve domain. We then map the 2D workspace $\mathcal{W}$ to $\mathcal{C}$ by using $\text{SF}^{-1}(\cdot)$.

Lemma 3 ([26]): Consider space-filling mapping $\text{SF}(\cdot)$. If the sensors are uniformly distributed in $\mathcal{W}$, they will be uniformly distributed in $\mathcal{C}$.

Let $\{\phi_i\}_{i=1}^N$ and $\{q_{\text{SF},i}\}_{i=1}^N$ denote the stop positions in $\mathcal{C}$ and their corresponding mappings in $\mathcal{W}$, respectively. Without

[5]The Voronoi partition $\{\mathcal{V}_i(\mathcal{Q})\}_{i=1}^N$ of the workspace $\mathcal{W}$ generated by a set of stop positions $\mathcal{Q}$ is defined as follows: $\mathcal{V}_i(\mathcal{Q}) = \{x \in \mathcal{W} | \|x - q_i\| \leq \|x - q_j\|, \forall\, i \neq j\}$, for all i. See [34] for more details on Voronoi diagrams.

[6]Note that in this paper, we use superscript $\star$ to denote the optimal value of the corresponding optimization problem.

This article has been accepted for publication in a future issue of this journal, but has not been fully edited. Content may change prior to final publication. Citation information: DOI 10.1109/TCNS.2016.2574129, IEEE Transactions on Control of Network Systems

loss of generality, we assume that $0 \leq \phi_1 \leq \phi_2 \cdots \leq \phi_N < 1$. Moreover, let $\Delta_{i-1,i} = \phi_i - \phi_{i-1}$, for $i \in \{2, \cdots, N\}$, be the length of the arc from ϕ_{i-1} to ϕ_i, and $\Delta_{N,1} = \phi_1 + 1 - \phi_N$ be the length of the arc from ϕ_N to ϕ_1. Note that $\sum_{i=2}^{N} \Delta_{i-1,i} + \Delta_{N,1} = 1$. Then, the total communication cost in $\mathcal{W}$ can be characterized as follows:

$$\begin{aligned}
&E_{\text{tot,comm,unif}}(N, \mathcal{Q}_{\text{SF}}, \{\mathcal{W}_{\text{SF},i}\}_{i=1}^{N}) \\
&= m \sum_{i=1}^{N} \int_{\mathcal{W}_{\text{SF},i}} \frac{1}{D^2} P_{\text{C}}(x, q_{\text{SF},i}) \frac{\rho T}{BR} dx \\
&\leq m \sum_{i=1}^{N} \int_{\text{SF}(\mathcal{C}_i)} \frac{1}{D^2} P_{\text{C}}(x, q_{\text{SF},i}) \frac{\rho T}{BR} dx \\
&\leq \frac{m\alpha(2^R - 1)\rho T}{KBR} \sum_{i=1}^{N} \int_{\mathcal{C}_i} C_{\text{SF}}^{n_{\text{PL}}} D^{n_{\text{PL}}} \left|\phi - \phi_i\right|^{\frac{n_{\text{PL}}}{2}} d\phi \\
&= \frac{m\alpha C_{\text{SF}}^{n_{\text{PL}}} D^{n_{\text{PL}}} (2^R - 1)\rho T}{KBR(n_{\text{PL}}/2 + 1) 2^{n_{\text{PL}}/2}} \left(\sum_{i=2}^{N} \Delta_{i-1,i}^{n_{\text{PL}}/2+1} + \Delta_{N,1}^{n_{\text{PL}}/2+1} \right),
\end{aligned} \tag{8}$$

where $E_{\text{tot,comm,unif}}(N, \mathcal{Q}_{\text{SF}}, \{\mathcal{W}_{\text{SF},i}\}_{i=1}^{N})$ is the total communication energy cost for the case of uniformly distributed sensors, $\mathcal{Q}_{\text{SF}} = \{q_{\text{SF},1}, \cdots, q_{\text{SF},N}\}$, $\{\mathcal{W}_{\text{SF},i}\}_{i=1}^{N}$ is the Voronoi partition generated by $\mathcal{Q}_{\text{SF}}$ in the 2D workspace, and $\{\mathcal{C}_i\}_{i=1}^{N}$ is the Voronoi partition generated by $\{\phi_i\}_{i=1}^{N}$ in the space-filling curve domain. Note that the first and second inequalities in (8) are obtained based on Lemma 2 and (1), respectively. Also, we can prove that the sensors in 1D are uniformly distributed by applying Lemma 3. This is then utilized in the third line of (8). Moreover, the boundary of the two neighboring Voronoi partitions in 1D can be easily obtained by choosing the middle point between the corresponding stop positions. Then, the last equality of (8) follows straightforwardly.

As can be seen, the upper bound of $E_{\text{tot,comm,unif}}(N, \mathcal{Q}_{\text{SF}}, \{\mathcal{W}_{\text{SF},i}\}_{i=1}^{N})$ is a convex function of $\Delta_{i-1,i}$ and $\Delta_{N,1}$, and is minimized by choosing $\Delta_{i-1,i}^{\star} = \Delta_{N,1}^{\star} = 1/N$, for $i \in \{2, \cdots, N\}$, i.e. the stop positions are chosen to be equally-spaced in the space-filling curve domain. Without loss of generality, we choose $\phi_i^{\star} = (2i-1)/(2N)$ and $q_{\text{SF},i}^{\star} = \text{SF}(\phi_i^{\star})$, for $i \in \{1, \cdots, N\}$. As a result, we have

$$\begin{aligned}
E_{\text{tot,SF,comm,unif}}(N) &= E_{\text{tot,comm,unif}}(N, \mathcal{Q}_{\text{SF}}^{\star}, \{\mathcal{W}_{\text{SF},i}^{\star}\}_{i=1}^{N}) \\
&\leq \frac{m\alpha C_{\text{SF}}^{n_{\text{PL}}} D^{n_{\text{PL}}} (2^R - 1)\rho T}{(n_{\text{PL}}/2 + 1)(2N)^{\frac{n_{\text{PL}}}{2}} KBR},
\end{aligned} \tag{9}$$

where $E_{\text{tot,SF,comm,unif}}(N)$ is the communication cost in the 2D workspace by using the above stop position selection strategy, $\mathcal{Q}_{\text{SF}}^{\star} = \{q_{\text{SF},1}^{\star}, \cdots, q_{\text{SF},N}^{\star}\}$, and $\{\mathcal{W}_{\text{SF},i}^{\star}\}_{i=1}^{N}$ is the Voronoi partition generated by $\mathcal{Q}_{\text{SF}}^{\star}$ (we know this is optimal from Lemma 2).

2) Optimization of the tour (variables $z_{i,j}$s and u_is): Next, consider the motion of the robot. Note that a minimum-distance tour will not be the optimal solution anymore. This is due to the fact that the robot needs to accelerate and decelerate between adjacent stop positions along the tour (there is an acceleration cost). Thus, the total motion cost not only depends on the total length of the tour, but also depends on the lengths of individual line segments. We next show that the minimum-length tour minimizes a tight upper bound on the motion cost if t_{mo} is not very small. More specifically, we consider an upper bound of (5) as follows:

$$E_{\text{mo,upper}}(d, t_{\text{mo}}) = \frac{\kappa_1 d^2}{t_{\text{mo}} - 2\sqrt{\kappa_3/\kappa_1}} + \kappa_2 d + \kappa_4 t_{\text{mo}}, \tag{10}$$

assuming $t_{\text{mo}} > 2\sqrt{\kappa_3/\kappa_1}$. Note that this bound is tight when t_{mo} is not close to zero. Without loss of generality, for a fixed given tour $\mathcal{T}$, we label the stop positions such that the robot visits them by the order of their labels. Then, the upper bound of the total motion cost is given by $E_{\text{tot,mo,upper}}(N, \mathcal{Q}, \{t_{\text{mo},i,i+1}\}_{i=1}^{N-1}, t_{\text{mo},N,1}, \mathcal{T}) = \sum_{i=1}^{N-1} E_{\text{mo,upper}}(\|q_{i+1} - q_i\|, t_{\text{mo},i,i+1}) + E_{\text{mo,upper}}(\|q_N - q_1\|, t_{\text{mo},N,1})$. We then have the following lemma.

Lemma 4: Given a fixed total motion time budget $T_{\text{mo}} > 2\sqrt{\kappa_3/\kappa_1}N$ and a fixed set of stop positions $\mathcal{Q}$, the optimal value of the following optimization problem is monotonically increasing with respect to the total travel distance $d_{\text{tot}}(\mathcal{Q}, \mathcal{T}) = \sum_{i=1}^{N-1} \|q_{i+1} - q_i\| + \|q_N - q_1\|$:

$$\begin{aligned}
\text{min.} \quad & E_{\text{tot,mo,upper}}(N, \mathcal{Q}, \{t_{\text{mo},i,i+1}\}_{i=1}^{N-1}, t_{\text{mo},N,1}, \mathcal{T}) \\
\text{s.t.} \quad & 1)\ t_{\text{mo},N,1} + \sum_{i=1}^{N-1} t_{\text{mo},i,i+1} \leq T_{\text{mo}}, \\
& 2)\ t_{\text{mo},i,i+1} \geq 2\sqrt{\kappa_3/\kappa_1}, \forall\, i, \quad t_{\text{mo},N,1} \geq 2\sqrt{\kappa_3/\kappa_1},
\end{aligned} \tag{11}$$

where $E_{\text{mo,upper}}(d, t_{\text{mo}})$ is defined to be ∞ if $t_{\text{mo}} = 2\sqrt{\kappa_3/\kappa_1}$.

Proof: It is easy to show that the optimization problem of (11) is convex. Then, the dual function of the primal problem is $g = \sum_{i=1}^{N-1} E_{\text{mo,upper}}(\|q_{i+1} - q_i\|, t_{\text{mo},i,i+1}) + E_{\text{mo,upper}}(\|q_N - q_1\|, t_{\text{mo},N,1}) + \lambda(t_{\text{mo},N,1} + \sum_{i=1}^{N-1} t_{\text{mo},i,i+1} - T_{\text{mo}}) - \sum_{i=1}^{N-1} \nu_{i,i+1}(t_{\text{mo},i,i+1} - 2\sqrt{\kappa_3/\kappa_1}) - \nu_{N,1}(t_{\text{mo},N,1} - 2\sqrt{\kappa_3/\kappa_1})$, where λ, $\nu_{i,i+1}$ and $\nu_{N,1}$ are Lagrange multipliers. Based on the Karush-Kuhn-Tucker (KKT) conditions [35], we have $\partial g/\partial t_{\text{mo},i,i+1} = -\kappa_1 \|q_{i+1} - q_i\|^2/(t_{\text{mo},i,i+1} - 2\sqrt{\kappa_3/\kappa_1})^2 + \lambda - \nu_{i,i+1} + \kappa_4 = 0$, for all i, and $\partial g/\partial t_{\text{mo},N,1} = -\kappa_1 \|q_N - q_1\|^2/(t_{\text{mo},N,1} - 2\sqrt{\kappa_3/\kappa_1})^2 + \lambda - \nu_{N,1} + \kappa_4 = 0$.

Since constraint 2 can never be active when $T_{\text{mo}} > 2\sqrt{\kappa_3/\kappa_1}N$, we have $\nu_{i,i+1}^{\star} = 0$, for all i, and $\nu_{N,1}^{\star} = 0$. Moreover, if $T_{\text{mo}} \geq \sqrt{\kappa_1/\kappa_4} d_{\text{tot}}(\mathcal{Q}, \mathcal{T}) + 2\sqrt{\kappa_3/\kappa_1}N$, we have $\lambda^{\star} = 0$, $t_{\text{mo},i,i+1}^{\star} = \sqrt{\kappa_1/\kappa_4}\|q_{i+1} - q_i\| + 2\sqrt{\kappa_3/\kappa_1}$, for all i, and $t_{\text{mo},N,1}^{\star} = \sqrt{\kappa_1/\kappa_4}\|q_N - q_1\| + 2\sqrt{\kappa_3/\kappa_1}$. As a result, the optimal value of (11) is

$$(2\sqrt{\kappa_1\kappa_4} + \kappa_2) d_{\text{tot}}(\mathcal{Q}, \mathcal{T}) + 2\kappa_4\sqrt{\kappa_3/\kappa_1}N, \tag{12}$$

which is monotonically increasing with respect to $d_{\text{tot}}(\mathcal{Q}, \mathcal{T})$. For the case where $2\sqrt{\kappa_3/\kappa_1}N < T_{\text{mo}} < \sqrt{\kappa_1/\kappa_4} \times d_{\text{tot}}(\mathcal{Q}, \mathcal{T}) + 2\sqrt{\kappa_3/\kappa_1}N$, it is straightforward to show that $t_{\text{mo},i,i+1}^{\star} = \|q_{i+1} - q_i\|(T_{\text{mo}} - 2\sqrt{\kappa_3/\kappa_1}N)/d_{\text{tot}}(\mathcal{Q}, \mathcal{T}) + 2\sqrt{\kappa_3/\kappa_1}$, for all i, and $t_{\text{mo},N,1}^{\star} = \|q_N - q_1\|(T_{\text{mo}} - 2\sqrt{\kappa_3/\kappa_1}N)/d_{\text{tot}}(\mathcal{Q}, \mathcal{T}) + 2\sqrt{\kappa_3/\kappa_1}$, resulting in the following optimal value:

$$\frac{\kappa_1 d_{\text{tot}}^2(\mathcal{Q}, \mathcal{T})}{T_{\text{mo}} - 2\sqrt{\kappa_3/\kappa_1}N} + \kappa_2 d_{\text{tot}}(\mathcal{Q}, \mathcal{T}) + \kappa_4 T_{\text{mo}}. \tag{13}$$

Clearly, the optimal value is monotonically increasing with respect to $d_{\text{tot}}(\mathcal{Q}, \mathcal{T})$, which completes the proof. ■

This article has been accepted for publication in a future issue of this journal, but has not been fully edited. Content may change prior to final publication. Citation information: DOI 10.1109/TCNS.2016.2574129, IEEE Transactions on Control of Network Systems

Lemma 4 shows that the minimum-distance tour minimizes the upper bound of the motion cost. Thus, we choose the minimum-distance tour to cover $\mathcal{Q}$ in 2D. Such a tour can be found by simply ordering the stop positions in the space-filling curve domain, as discussed in Section II-A.

3) Optimization of the motion times (variables $t_{\mathrm{mo},i,i+1}$s and $t_{\mathrm{mo},N,1}$): Based on the previous stop position selection and path planning strategy, the remaining variables to solve for are the number of clusters and the motion times. Then, the optimization problem of (6) can be simplified as follows:

$$\begin{aligned}\min.\quad & E_{\text{tot,SF,unif}}(N,\{t_{\mathrm{mo},i,i+1}\}_{i=1}^{N-1},t_{\mathrm{mo},N,1})\\ &= E_{\text{tot,unif}}(N,\mathcal{Q}^\star_{\text{SF}},\{\mathcal{W}^\star_{\text{SF},i}\}_{i=1}^{N},\{t_{\mathrm{mo},i,j}\}_{i,j=1}^{N},\mathcal{T}^\star_{\text{SF}})\\ &= \underbrace{m\sum_{i=1}^{N}\int_{\mathcal{W}^\star_{\text{SF},i}}\frac{1}{D^2}P_{\text{C}}(x,q^\star_{\text{SF},i})\frac{\rho T}{BR}dx}_{E_{\text{tot,SF,comm,unif}}(N)}\\ &\quad+\varpi\underbrace{\left(\sum_{i=1}^{N-1}E_{\mathrm{mo}}(\|q^\star_{\text{SF},i+1}-q^\star_{\text{SF},i}\|,t_{\mathrm{mo},i,i+1})\right.}\\ &\qquad\left.+E_{\mathrm{mo}}(\|q^\star_{\text{SF},N}-q^\star_{\text{SF},1}\|,t_{\mathrm{mo},N,1})\right)\\ &\qquad\qquad\qquad\qquad\qquad\qquad(14)\\ &\qquad\underbrace{\qquad\qquad\qquad\qquad}_{\substack{E_{\text{tot,SF,mo}}(N,\{t_{\mathrm{mo},i,i+1}\}_{i=1}^{N-1},t_{\mathrm{mo},N,1})\\=E_{\text{tot,mo}}(N,\mathcal{Q}^\star_{\text{SF}},\{t_{\mathrm{mo},i,j}\}_{i,j=1}^{N},\mathcal{T}^\star_{\text{SF}})}}\\ \text{s.t.}\quad & 1)\ \sum_{i=1}^{N-1}t_{\mathrm{mo},i,i+1}+t_{\mathrm{mo},N,1}\le T\left(1-\frac{m\rho}{BR}\right),\\ & 2)\ t_{\mathrm{mo},i,i+1}\ge 0,\forall\, i,\quad t_{\mathrm{mo},N,1}\ge 0,\end{aligned}$$

where $E_{\text{tot,unif}}(N,\mathcal{Q}^\star_{\text{SF}},\{\mathcal{W}^\star_{\text{SF},i}\}_{i=1}^{N},\{t_{\mathrm{mo},i,j}\}_{i,j=1}^{N},\mathcal{T}^\star_{\text{SF}})$ is the total cost for the case of uniformly distributed sensors, $\mathcal{T}^\star_{\text{SF}}$ is the minimum-distance tour obtained by ordering the stop positions in the space-filling curve domain, and $E_{\text{tot,SF,unif}}(N,\{t_{\mathrm{mo},i,i+1}\}_{i=1}^{N-1},t_{\mathrm{mo},N,1})$ and $E_{\text{tot,SF,mo}}(N,\{t_{\mathrm{mo},i,i+1}\}_{i=1}^{N-1},t_{\mathrm{mo},N,1})$ denote the total cost and total motion cost in the 2D workspace, respectively, based on the stop position selection and path planning strategy in the space-filling curve domain. For a fixed N, equation (14) becomes a convex optimization problem since $E_{\text{tot,SF,mo}}(N,\{t_{\mathrm{mo},i,i+1}\}_{i=1}^{N-1},t_{\mathrm{mo},N,1})$ is a convex function of the motion times (as shown in Lemma 1).

4) Optimization of the number of clusters (variable N): Finally, we find the best N by characterizing (14) for integer Ns up to $N_{\max}$ and finding where the minimum occurs. We show how to choose $N_{\max}$ in Section III-B.

We then propose Algorithm 1 for the initial phase of our framework. More specifically, we first find the cost for the case of no clustering. Then, we solve (14) for each $N\in\{2,\cdots,N_{\max}\}$ to obtain $E^\star_{\text{tot,SF,unif}}(N)$, where $E^\star_{\text{tot,SF,unif}}(N)$ is the optimal value of (14) for a fixed N, and $N_{\max}$ is the maximum number of clusters (more discussions on $N_{\max}$ in Section III-B). Next, we find $N^\star$ by minimizing $E^\star_{\text{tot,SF,unif}}(N)$, for $N\in\{1,\cdots,N_{\max}\}$, with $E^\star_{\text{tot,SF,unif}}(N=1)=E^\star_{\text{tot,noCl,unif}}$. If $N^\star=1$, we do not cluster the workspace and choose the center of the workspace as the only stop position. Otherwise, we choose the stop positions as the mapping of the $N^\star$ equally-spaced points in the space-filling curve domain. The tour is also readily given by ordering the stop positions in the space-filling curve domain. The clustering is then obtained by the Voronoi partition generated by the stop positions in $\mathcal{W}$. Finally, the motion times are given by the optimal solution of (14) for $N=N^\star$.

Algorithm 1 Our proposed approach: Initial phase

```
find E*_{tot,noCl,unif} by using (7)
solve (14), for N ∈ {2, ··· , N_max}
find N* that minimizes E*_{tot,SF,unif}(N)
if N* = 1
    return no clustering
else
    choose N* equally-spaced stop positions in C
    find the tour by ordering the stop positions
    map the stop positions and the tour from C to W
    choose the clusters to be the Voronoi partition
      generated by the stop positions in W
    use the corresponding optimal solution of (14) for the
      motion times
end
```

B. Upper Bound Derivation

Since the stop positions are equally-spaced in the space-filling curve domain, the distance between the neighboring stop positions in 2D is bounded from above by $C_{\text{SF}}D/\sqrt{N}$ using (1). As a result, the total distance of the tour in the 2D workspace is bounded from above by $C_{\text{SF}}D\sqrt{N}$. Hence, based on the proof of Lemma 4, if $BR>m\rho$ and T satisfies $(1-m\rho/(BR))T\ge\sqrt{\kappa_1/\kappa_4}C_{\text{SF}}D\sqrt{N}+2\sqrt{\kappa_3/\kappa_1}N$, we then have the following upper bound for the total motion cost:

$$\begin{aligned}E_{\text{tot,SF,mo}}(N,\{t^\star_{\mathrm{mo},i,i+1}\}_{i=1}^{N-1},t^\star_{\mathrm{mo},N,1})&<\kappa_{\mathrm{M},1}C_{\text{SF}}D\sqrt{N}\\&\quad+\kappa_{\mathrm{M},2}N<(\kappa_{\mathrm{M},1}C_{\text{SF}}D+\kappa_{\mathrm{M},2})N,\end{aligned}\tag{15}$$

where $t^\star_{\mathrm{mo},i,i+1}$, for all i, and $t^\star_{\mathrm{mo},N,1}$ are the optimal motion times obtained by solving (14), $\kappa_{\mathrm{M},1}=2\sqrt{\kappa_1\kappa_4}+\kappa_2$ and $\kappa_{\mathrm{M},2}=2\kappa_4\sqrt{\kappa_3/\kappa_1}$. Moreover, the upper bound for the communication cost is given by (9). Then, the optimal solution of (14) for a fixed N is bounded from above by

$$\begin{aligned}E^\star_{\text{tot,SF,unif}}(N)&<E_{\text{tot,SF,unif,upper}}(N)\\&=\frac{m\alpha C_{\text{SF}}^{n_{\text{PL}}}D^{n_{\text{PL}}}(2^R-1)\rho T}{(n_{\text{PL}}/2+1)(2N)^{\frac{n_{\text{PL}}}{2}}KBR}\\&\quad+\varpi(\kappa_{\mathrm{M},1}C_{\text{SF}}D+\kappa_{\mathrm{M},2})N.\end{aligned}\tag{16}$$

Note that the exact communication and motion costs in the 2D workspace are not strictly decreasing and increasing with respect to N, respectively. As a consequence, it is challenging to select an $N_{\max}$ to ensure that there is no $N\ge N_{\max}+1$ that can result in a smaller $E^\star_{\text{tot,SF,unif}}(N)$. However, as can be seen, their upper bounds (9) and (15), which are obtained by using (1), do have the corresponding monotonic properties. Hence, we can use (16) to find an appropriate $N_{\max}$.

Note that although N is subject to an integer constraint $N\in\{2,3,\cdots\}$, $E_{\text{tot,SF,unif,upper}}(N_c)$ is a convex function of

This article has been accepted for publication in a future issue of this journal, but has not been fully edited. Content may change prior to final publication. Citation information: DOI 10.1109/TCNS.2016.2574129, IEEE Transactions on Control of Network Systems

N_c for a continuous $N_c \in [2, \infty)$. As a result, it can be shown that:

$$N_c^\star = \begin{cases} \frac{1}{2}\left(\frac{n_{\text{PL}} m\alpha C_{\text{SF}}^{n_{\text{PL}}} D^{n_{\text{PL}}}(2^R-1)\rho T}{(n_{\text{PL}}/2+1)KBR\varpi(\kappa_{\text{M},1}C_{\text{SF}}D+\kappa_{\text{M},2})}\right)^{\frac{2}{n_{\text{PL}}+2}}, \\ \text{if } \left(\frac{n_{\text{PL}} m\alpha C_{\text{SF}}^{n_{\text{PL}}} D^{n_{\text{PL}}}(2^R-1)\rho T}{(n_{\text{PL}}/2+1)KBR\varpi(\kappa_{\text{M},1}C_{\text{SF}}D+\kappa_{\text{M},2})}\right)^{\frac{2}{n_{\text{PL}}+2}} \geq 4, \\ 2, \quad \text{otherwise.} \end{cases} \tag{17}$$

Then, the optimal $N^\star$ that minimizes $E_{\text{tot,SF,unif,upper}}(N)$, for $N \in \{2, 3, \cdots\}$, can be found as

$$N^\star = \underset{N\in\{\lfloor N_c^\star \rfloor, \lceil N_c^\star \rceil\}}{\arg\min} \{E_{\text{tot,SF,unif,upper}}(N)\}. \tag{18}$$

A good choice of $N_{\max}$ is $\lceil N_c^\star \rceil$ for the following reason. Note that both (9) and (15) depend on inequality (1). Moreover, since the communication cost is an integral of a polynomial of order n_{PL} of the distance (see the first line of (8)), the error of the approximation is expected to be more amplified in (9), as compared to (15). This results in an overestimation of N. We thus expect $\lceil N_c^\star \rceil$ to be larger than the optimum $N^\star$ that minimizes $E_{\text{tot,SF,unif}}^\star(N)$ with a high probability.

Theorem 1: If $BR > m\rho$ and the total time budget T is sufficiently large, such that

$$T \geq \frac{2^{n_{\text{PL}}+2}(n_{\text{PL}}/2+1)KBR\varpi(\kappa_{\text{M},1}C_{\text{SF}}D+\kappa_{\text{M},2})}{n_{\text{PL}} m\alpha C_{\text{SF}}^{n_{\text{PL}}} D^{n_{\text{PL}}}(2^R-1)\rho}, \tag{19}$$

and

$$T \geq \frac{\sqrt{\kappa_1/\kappa_4}C_{\text{SF}}D\sqrt{\lceil N_c^\star \rceil} + 2\sqrt{\kappa_3/\kappa_1}\lceil N_c^\star \rceil}{1 - m\rho/(BR)}. \tag{20}$$

We have the following upper bound for the optimal total cost $E_{\text{tot,SF,unif}}^\star = \min_{N\in\{2,3,\cdots\}}\{E_{\text{tot,SF,unif}}^\star(N)\}$:

$$\begin{aligned} E_{\text{tot,SF,unif}}^\star < E_{\text{tot,SF,unif,upper}}^\star &< \left(\frac{n_{\text{PL}}}{n_{\text{PL}}/2+1}\right)^{\frac{2}{n_{\text{PL}}+2}} \left(\frac{1}{n_{\text{PL}}}+\frac{3}{4}\right) \\ &\times \varpi^{\frac{n_{\text{PL}}}{n_{\text{PL}}+2}} (\kappa_{\text{M},1}C_{\text{SF}}D+\kappa_{\text{M},2})^{\frac{n_{\text{PL}}}{n_{\text{PL}}+2}} \\ &\times \left(\frac{m\alpha C_{\text{SF}}^{n_{\text{PL}}} D^{n_{\text{PL}}}(2^R-1)\rho T}{KBR}\right)^{\frac{2}{n_{\text{PL}}+2}}, \end{aligned} \tag{21}$$

where $E_{\text{tot,SF,unif,upper}}^\star = \min_{N\in\{2,3,\cdots\}}\{E_{\text{tot,SF,unif,upper}}^\star(N)\}$. Moreover, compared to the case of no clustering, we have

$$\begin{aligned} \frac{E_{\text{tot,SF,unif}}^\star}{E_{\text{tot,noCl,unif}}^\star} < \frac{E_{\text{tot,SF,unif,upper}}^\star}{E_{\text{tot,noCl,unif}}^\star} &< \frac{C_{\text{SF}}^{\frac{2n_{\text{PL}}}{n_{\text{PL}}+2}}}{C_1}\left(\frac{n_{\text{PL}}}{n_{\text{PL}}/2+1}\right)^{\frac{2}{n_{\text{PL}}+2}} \\ \times \left(\frac{1}{n_{\text{PL}}}+\frac{3}{4}\right)&\left(\frac{\varpi(\kappa_{\text{M},1}C_{\text{SF}}D+\kappa_{\text{M},2})KBR}{m\alpha D^{n_{\text{PL}}}(2^R-1)\rho T}\right)^{\frac{n_{\text{PL}}}{n_{\text{PL}}+2}}. \end{aligned} \tag{22}$$

Proof: Note that if $BR > m\rho$, and (19) and (20) are satisfied, then $N_c^\star \geq 2$ and $E_{\text{tot,SF,unif}}^\star(N)$ is bounded from above by $E_{\text{tot,SF,unif,upper}}(N)$ when choosing $N = \lceil N_c^\star \rceil$. Then, we have the following upper bound for $E_{\text{tot,SF,unif}}^\star$:

$$\begin{aligned} E_{\text{tot,SF,unif}}^\star &< E_{\text{tot,SF,unif,upper}}^\star \leq E_{\text{tot,SF,unif,upper}}(\lceil N_c^\star \rceil) \\ &= \frac{m\alpha C_{\text{SF}}^{n_{\text{PL}}} D^{n_{\text{PL}}}(2^R-1)\rho T}{(n_{\text{PL}}/2+1)(2\lceil N_c^\star \rceil)^{\frac{n_{\text{PL}}}{2}} KBR} \\ &\qquad + \varpi(\kappa_{\text{M},1}C_{\text{SF}}D+\kappa_{\text{M},2})\lceil N_c^\star \rceil \\ &< \frac{m\alpha C_{\text{SF}}^{n_{\text{PL}}} D^{n_{\text{PL}}}(2^R-1)\rho T}{(n_{\text{PL}}/2+1)(2N_c^\star)^{\frac{n_{\text{PL}}}{2}} KBR} \\ &\qquad + \frac{3}{2}\varpi(\kappa_{\text{M},1}C_{\text{SF}}D+\kappa_{\text{M},2})N_c^\star \\ &= \left(\frac{n_{\text{PL}}}{n_{\text{PL}}/2+1}\right)^{\frac{2}{n_{\text{PL}}+2}} \left(\frac{1}{n_{\text{PL}}}+\frac{3}{4}\right)(\kappa_{\text{M},1}C_{\text{SF}}D+\kappa_{\text{M},2})^{\frac{n_{\text{PL}}}{n_{\text{PL}}+2}} \\ &\qquad \times \varpi^{\frac{n_{\text{PL}}}{n_{\text{PL}}+2}} \left(\frac{m\alpha C_{\text{SF}}^{n_{\text{PL}}} D^{n_{\text{PL}}}(2^R-1)\rho T}{KBR}\right)^{\frac{2}{n_{\text{PL}}+2}}, \end{aligned}$$

where the third inequality follows from the fact that the first and second terms of $E_{\text{tot,SF,unif,upper}}(N)$ are monotonically decreasing and monotonically increasing with respect to N respectively, for $N \geq 2$. This confirms (21).

Equation (22) can be easily obtained by substituting the upper bound of (21) into $E_{\text{tot,SF,unif,upper}}^\star / E_{\text{tot,noCl,unif}}^\star$. ■

Interpretation of the results: It can be seen from Theorem 1 that the upper bound of $E_{\text{tot,SF,unif}}^\star / E_{\text{tot,noCl,unif}}^\star$ depends on $\varpi(\kappa_{\text{M},1}C_{\text{SF}}D + \kappa_{\text{M},2})KBR/(m\alpha D^{n_{\text{PL}}}(2^R-1)\rho T)$. Hence, the upper bound decreases if the motion cost $(\kappa_{\text{M},1}D + \kappa_{\text{M},2})$ decreases and/or the number of information bits generated in each period $(m\rho T)$ increases. Also, the upper bound decreases as σ_{dB}^2 increases, since α is monotonically increasing with respect to σ_{dB}^2. These observations are intuitive, since as the communication demand (the total number of generated information bits in each period) becomes higher and/or the predicted channel quality gets worse, more clustering is preferred in order to reduce the communication cost, as shown in (17). As a result, the robot will save more energy, as compared to the case of no clustering.

It is worth to note that although both sides of (20) depend on T, we can always find a large enough T to satisfy this condition. This is because the increasing order of the right-hand side of (20) is $T^{2/(n_{\text{PL}}+2)}$, which is smaller than the increasing order of the left hand side.

IV. Proposed Iterative Approach for Joint Clustering and Path Planning

In this part, we finalize the co-design of our clustering and path planning in realist communication environments. More specifically, by utilizing our initial design phase and Lloyd's algorithm [34], we propose an iterative approach to fine tune the initial design.

We first choose N and initialize variables $\mathcal{Q}$, $\{\mathcal{W}_i\}_{i=1}^N$, $\{t_{\text{mo},i,j}\}_{i,j=1}^N$ and $\mathcal{T}$ in (6) by using the solution obtained from Algorithm 1. Then, we fix N and optimize the rest of the variables in an iterative way as follows. In each iteration, we first optimize $\mathcal{Q}$ in (6) for fixed $\{\mathcal{W}_i^{(k)}\}_{i=1}^N$, $\{t_{\text{mo},i,j}^{(k)}\}_{i,j=1}^N$ and $\mathcal{T}^{(k)}$ to obtain a new set of stop positions $\mathcal{Q}^{(k+1)}$, where superscript k denotes that the variables are obtained after the k^{th} iteration. Note that we have a convex optimization problem

This article has been accepted for publication in a future issue of this journal, but has not been fully edited. Content may change prior to final publication. Citation information: DOI 10.1109/TCNS.2016.2574129, IEEE Transactions on Control of Network Systems

Algorithm 2 Proposed iterative approach

1: initialize $\mathcal{Q}^{(1)}$, $\{\mathcal{W}_i^{(1)}\}_{i=1}^N$, $\{t_{\text{mo},i,j}^{(1)}\}_{i,j=1}^N$ and $\mathcal{T}^{(1)}$ by using Algorithm 1
2: for $k = 1, 2, \cdots$
3: optimize $\mathcal{Q}$ for fixed $\{\mathcal{W}_i^{(k)}\}_{i=1}^N$, $\{t_{\text{mo},i,j}^{(k)}\}_{i,j=1}^N$ and $\mathcal{T}^{(k)}$ to obtain $\mathcal{Q}^{(k+1)}$
4: find Voronoi partition $\{\mathcal{W}_i^{(k+1)}\}_{i=1}^N$ for fixed $\mathcal{Q}^{(k+1)}$
5: find a new tour $\mathcal{T}^{(k+1)}$ for fixed $\mathcal{Q}^{(k+1)}$
6: optimize $\{t_{\text{mo},i,j}\}_{i,j=1}^N$ for fixed $Q^{(k+1)}$, $\{\mathcal{W}_i^{(k+1)}\}_{i=1}^N$ and $\mathcal{T}^{(k+1)}$ to obtain $\{t_{\text{mo},i,j}^{(k+1)}\}_{i,j=1}^N$
7: if the total cost increases as compared to the last iteration
8: reject the new TSP solution and assign $\mathcal{T}^{(k+1)} = \mathcal{T}^{(k)}$
9: optimize $\{t_{\text{mo},i,j}\}_{i,j=1}^N$ again for fixed $Q^{(k+1)}$, $\{\mathcal{W}_i^{(k+1)}\}_{i=1}^N$ and $\mathcal{T}^{(k+1)}$
10: end
11: if the energy no longer decreases
12: break
13: end
14: end

at this step, which guarantees to have a unique solution. Next, we choose $\{\mathcal{W}_i^{(k+1)}\}_{i=1}^N$ to be the Voronoi partition that is generated by $\mathcal{Q}^{(k+1)}$. Moreover, we find the new TSP tour $\mathcal{T}^{(k+1)}$ for $\mathcal{Q}^{(k+1)}$. Note that we can use space-filling curves or other heuristic approaches [28], [29] to solve the TSP problem sub-optimally but efficiently, as discussed in Section II-A. Finally, we solve $\{t_{\text{mo},i,j}\}_{i,j=1}^N$ in (6) for fixed $\mathcal{Q}^{(k+1)}$, $\{\mathcal{W}_i^{(k+1)}\}_{i=1}^N$ and $\mathcal{T}^{(k+1)}$, which is also a convex optimization problem. It is worth to note that $\mathcal{T}^{(k+1)}$ may have a longer total distance as compared to $\mathcal{T}^{(k)}$. Moreover, even if $\mathcal{T}^{(k+1)}$ has a shorter total distance, it is possible that the total cost after optimizing $\{t_{\text{mo},i,j}\}_{i,j=1}^N$ will become larger than the one obtained in the last iteration. This is because in general the motion cost is not monotonically decreasing with respect to the total distance of the tour, as discussed in Section III-A. To guarantee that our algorithm always reduces the total cost, we accept the new TSP solution only if it reduces the total cost as compared to the last iteration. Otherwise, we reject the new TSP solution, assigning $\mathcal{T}^{(k+1)} = \mathcal{T}^{(k)}$ and solving $\{t_{\text{mo},i,j}\}_{i,j=1}^N$ again. The algorithm repeats these steps until the total cost no longer decreases. We have summarized the proposed approach in Algorithm 2.

V. Extension to the Case of Non-uniformly Distributed Sensors

So far, we have considered the case where the sensors are uniformly distributed. As a result, we can choose the stop positions such that they are equally-spaced in the space-filling curve domain. In this part, we extend our previous framework to the case where the sensors are not uniformly distributed.

It is intuitive to expect that the optimal number of clusters in each area of the workspace increases as the density of the sensors in the corresponding area increases, in order to save the communication cost. Hence, we extend the first part of the framework in Section III-A as follows, in order to add more stop positions to the workspace as needed.[7] We first find the optimal cost for the case where there is no clustering by solving the following optimization problem:

$$\begin{aligned} \text{min.} \quad & E_{\text{tot,noCl,non-unif}}(q_1) \\ & = \frac{m\alpha(2^R-1)\rho T}{KBR}\int_{\mathcal{W}} p(x)\|x-q_1\|^{n_{\text{PL}}}dx \qquad (23) \\ \text{s.t.} \quad & 1)\ q_1 \in \mathcal{W}, \end{aligned}$$

where $E_{\text{tot,noCl,non-unif}}(q_1)$ denotes the cost for the case of no clustering when the sensors are not uniformly distributed and q_1 is the stop position of the robot. Unlike the uniform case, the optimal $q_1^\star$ in (23) depends on $p(x)$ and is not necessary the center of the workspace. It is straightforward to see that the objective function is a convex function of q_1 for typical path loss exponents $n_{\text{PL}} \in [2, 6]$. As a result, we can easily find the global optimum of (23).

Similar to Section III-A, for the case of more than one cluster, we determine the number of clusters and the corresponding stop positions by using space-filling curves as follows. First, we map the workspace (including the optimal $q_1^\star$ in (23)) to 1D. Without loss of generality, let $\text{SF}^{-1}(q_1^\star) = 0$. Next, we choose an additional stop position at 0.5 in 1D and map it back to the 2D workspace. Similar to the approach proposed in Section III-A, we then solve the following convex optimization problem for $N = 2$:

$$\begin{aligned} \text{min.} \quad & E_{\text{tot,SF,non-unif}}(\{t_{\text{mo},i,i+1}\}_{i=1}^{N-1}, t_{\text{mo},N,1}) = \\ & \frac{m\alpha(2^R-1)\rho T}{KBR}\sum_{i=1}^{N}\int_{\mathcal{W}_{\text{SF},i}} p(x)\|x-q_{\text{SF},i}\|^{n_{\text{PL}}}dx \\ & + \varpi\Bigg(E_{\text{mo}}(d_{N,1}, t_{\text{mo},N,1}) \\ & \qquad + \sum_{i=1}^{N-1} E_{\text{mo}}(d_{i,i+1}, t_{\text{mo},i,i+1})\Bigg) \qquad (24) \\ \text{s.t.} \quad & 1)\ \sum_{i=1}^{N-1} t_{\text{mo},i,i+1} + t_{\text{mo},N,1} \le T\left(1-\frac{m\rho}{BR}\right), \\ & 2)\ t_{\text{mo},i,i+1} \ge 0, \forall\, i, \quad t_{\text{mo},N,1} \ge 0, \end{aligned}$$

where $E_{\text{tot,SF,non-unif}}(\{t_{\text{mo},i,i+1}\}_{i=1}^{N-1}, t_{\text{mo},N,1})$ is the total cost when the sensors are not uniformly distributed. Here, the variables to solve for are $\{t_{\text{mo},i,i+1}\}_{i=1}^{N-1}$ and $t_{\text{mo},N,1}$. Note that without loss of generality, we label the stop positions such that the robot visits them by the order of their labels in (24). Also, we have $q_{\text{SF},1} = q_1^\star$ and $q_{\text{SF},2} = \text{SF}(0.5)$ for $N = 2$. We then compare the optimal value of (24) to the case of no clustering. If it has a larger cost, we do not cluster the workspace and terminate the algorithm. Otherwise, we keep this additional stop position. Since it is potentially beneficial to have more clusters in some areas of the workspace, we keep adding stop positions as follows. For the arc $[0, 0.5)$, we further choose

[7] Note that solving this problem optimally is not possible. Furthermore, exactly extending the approach in the previous part is not possible either, since the distribution in 1D is not known for a given non-uniform distribution in 2D. We therefore propose an iterative extension of the proposed approach of the uniform case.

This article has been accepted for publication in a future issue of this journal, but has not been fully edited. Content may change prior to final publication. Citation information: DOI 10.1109/TCNS.2016.2574129, IEEE Transactions on Control of Network Systems

0.25 as an additional stop position and map it back to the 2D workspace. We then find the path of the robot and solve (24) again for this new clustering strategy. If it does not increase the total cost, we then keep this new stop position along this arc. Otherwise, we do not choose this new stop position. We use the same strategy for the arc $[0.5, 1)$. Our algorithm stops if no arc between the existing adjacent stop positions needs new stop positions. We summarize our approach in Algorithm 3, where $\mathcal{E}$ and $\mathcal{E}_{\text{new}}$ denote the sets that contain all the arcs at the current and next steps of the algorithm respectively, $\mathcal{F}$ is the set that contains all the stop positions, and bool_{div} is a boolean variable to determine if we need to keep adding new stop positions.

Algorithm 3 Extension to the case of non-uniformly distributed sensors

find $E^{\star}_{\text{tot,noCl,non-unif}}$ by solving (23)
let $\mathcal{E} = \{\mathcal{C}\}$, $\mathcal{F} = \{\text{SF}^{-1}(q_1^{\star})\}$
set bool_{div} to be true
while bool_{div} is true
  set bool_{div} to be false
  for each arc in $\mathcal{E}$
    choose the center of the arc as an additional stop position for this arc
    find the TSP tour and map the stop position to 2D
    solve (24)
    if the optimal value of (24) does not increase
      divide the arc in half and add the resulting two sub-arcs to $\mathcal{E}_{\text{new}}$
      add the additional stop position to $\mathcal{F}$
      set bool_{div} to be true
    else
      add the original arc to $\mathcal{E}_{\text{new}}$
    end
  end
  set $\mathcal{E}$ to be $\mathcal{E}_{\text{new}}$
end
use the corresponding optimal solution of (24) for the motion times

As compared to Algorithm 1, the main difference of Algorithm 3 is that it adds stop positions to the parts of the workspace that can benefit from more clustering. This is intuitive since it is only beneficial to travel a longer distance in the areas that have a larger sensor density. As a result, our proposed algorithm will result in a clustering strategy that depends on $p(x)$. After using Algorithm 3, we then proceed with Algorithm 2 to fine tune the solution.

Remark 3: In general, finding the upper bound for the case of non-uniformly distributed sensors is very challenging. This is because, given an arbitrary distribution of sensors in the 2D workspace, its corresponding distribution in the space-filling curve domain cannot be easily obtained. Characterizing the upper bound for arbitrarily distributed sensors is thus a subject of our future work.

VI. Simulation Results

Consider the case where the workspace is a 1000 m $\times$ 1000 m square region with a total of 500 fixed sensors. The channel in the workspace has the following realistic channel parameters [36]: $n_{\text{PL}} = 4.57$ and $\sigma^2_{\text{dB}} = 64$. Moreover, we choose $R = 2$ bits/Hz/s, $p_{b,\text{th}} = 10^{-6}$, $B = 500$ MHz and the receiver noise power is chosen to be the realistic value of -204 dBW/Hz. We also use real motion parameters as follows [31]: $\kappa_1 = 0.77$, $\kappa_2 = 10.1$, $\kappa_3 = 5.47$ and $\kappa_4 = 4.24$. Furthermore, we use Sierpiński curves. Finally, we choose $\varpi = 0.1$, a sensing rate of $\rho = 0.8$ Mbps for each sensor and $T = 3600$ s.

Fig. 4 (left) shows the clusters of the sensors, the stop positions and the tour of the robot by using our proposed framework for the case where the sensors are uniformly distributed. As can be seen, in general, the stop positions are uniformly-spaced in the workspace. Still, the number of clusters, clustering, path planning and motion times need to be jointly optimized as we proposed in this paper. In this example, the predicted total cost of the whole network is only 1.2% of the energy cost of the case of no clustering, indicating a considerable energy saving achieved through proper co-optimization. In terms of computational cost, our MATLAB simulation for Fig. 4 (left) took 83.9 seconds to run on a 2.0 GHz CPU.

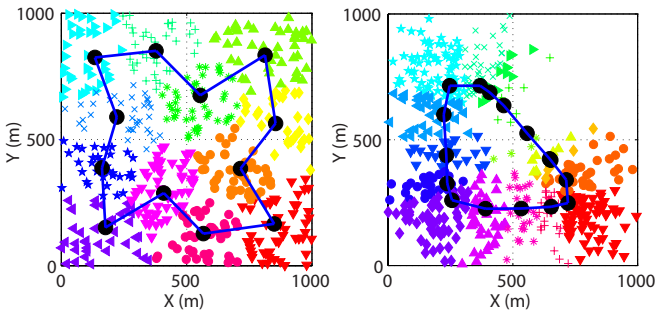

Fig. 4. The clusters of the sensors, the stop positions and the tours of the robot when the sensors are uniformly distributed (left) and non-uniformly distributed according to $p(x)$ (right), respectively. The figures show the results by using our proposed framework. The black circles and blue line segments indicate the stop positions and the tours of the robot, respectively. The markers with the same shape and color denote the same cluster. In these examples, the predicted total cost of the whole network is only 1.2% and 9.7% of the cost of the case of no clustering, respectively. See the pdf file for a color version.

Fig. 5 and Fig. 6 show the benefits of our proposed framework when the sensors are uniformly distributed. We compare our proposed framework to the case of no clustering (Fig. 5) as well as to the case where the robot needs to visit each sensor to collect the data (Fig. 6). For the second case, we first use space-filling curves to plan the tour of the robot. Then, we optimize the motion strategy of the robot for this fixed tour. It can be seen that our approach can save the energy considerably as compared to both of these benchmarks. Furthermore, as compared to the case of no clustering, our proposed framework becomes more beneficial as the communication cost becomes more dominant, i.e. the sensing rate or channel variance is higher. On the other hand, as compared to the case of visiting each sensor, our proposed framework becomes more beneficial

This article has been accepted for publication in a future issue of this journal, but has not been fully edited. Content may change prior to final publication. Citation information: DOI 10.1109/TCNS.2016.2574129, IEEE Transactions on Control of Network Systems

as the motion cost becomes more dominant, i.e. the sensing rate or channel variance becomes lower.

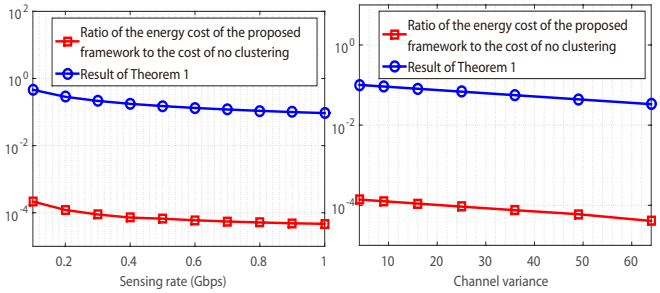

Fig. 5. The figure shows the ratio of the cost of our proposed framework to the cost of the case of no clustering, for different sensing rates (left) and different channel variances (right) when the sensors are uniformly distributed. The channel variance is 64 for the left figure and the sensing rate is 0.8 Gbps for the right figure. It can be seen that our framework can reduce the total cost considerably, as compared to the case of no clustering. The figure also shows the derived upper bound of Theorem 1.

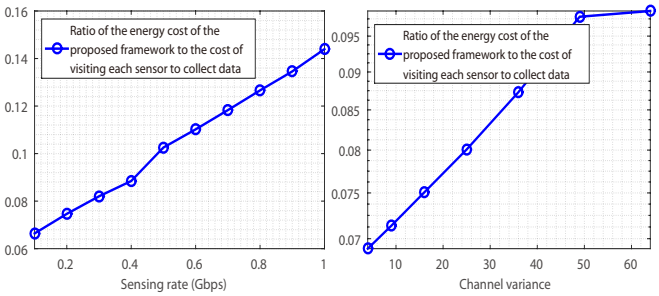

Fig. 6. The figure shows the ratio of the cost of our proposed framework to the cost of the case of visiting each sensor, for different sensing rates (left) and different channel variances (right) when the sensors are uniformly distributed. The channel variance is 64 for the left figure and the sensing rate is 0.8 Gbps for the right figure. It can be seen that our framework can reduce the total cost considerably, as compared to the case of visiting all the sites.

Fig. 4 (right) shows the result when the sensors are not uniformly distributed. In this example, we have $\rho = 80$ Kbps for each sensor and $p(x) = \widetilde{p}(x)/\int_{\mathcal{W}} \widetilde{p}(x)dx$, where

$$\widetilde{p}(x) = \sum_{i=1}^{3} \mathbb{I}(\pi = i)\mathcal{N}\left(\eta_i, \begin{bmatrix} 125 & 0 \\ 0 & 125 \end{bmatrix}\right).$$

Here, $\eta_1 = [250\ 250]^{\mathrm{T}}$, $\eta_2 = [750\ 250]^{\mathrm{T}}$, $\eta_3 = [250\ 750]^{\mathrm{T}}$, $\mathbb{I}(\cdot)$ denotes an indicator function, $\mathcal{N}(\cdot,\cdot)$ represents a Gaussian distribution with the first and second parameters denoting its mean and covariance respectively, and π denotes a generalized Bernoulli random variable where $\pi = i$ with probability 1/3 for all i. Fig. 4 (right) then shows the results of our proposed approach. It can be seen that we have more clusters in the areas where the density of the sensors is higher, as expected. Moreover, the predicted total cost of the whole network is only 9.7% of the cost of the case of no clustering, indicating a considerable energy saving achieved through proper co-optimization. In terms of computational cost, our MATLAB simulation for Fig. 4 (right) took 73.2 seconds to run on a 2.0 GHz CPU.

Fig. 7 (left and right) shows the benefits of our approach for different sensing rates and different channel variances respectively, when the sensors are distributed according to $p(x)$. Similar to the uniform case, as compared to the case of no clustering, our proposed approach becomes more beneficial as the communication cost becomes higher. On the other hand, as compared to the case of visiting each sensor, our proposed framework becomes more beneficial as the communication cost becomes lower.

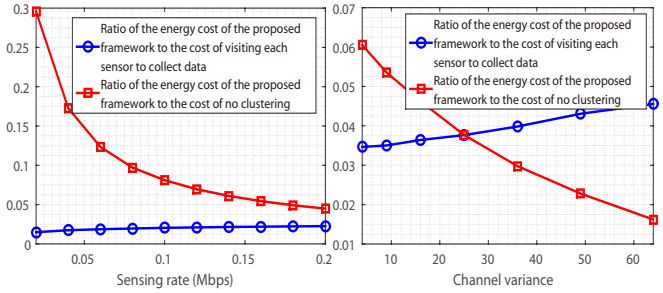

Fig. 7. The figure shows the ratio of the cost of our framework to the cost of the case of no clustering as well as to the cost of the case of visiting each sensor, for different sensing rates (left) and different channel variances (right) when the sensors are distributed according to $p(x)$. The channel variance is 64 for the left figure and the sensing rate is 1 Mbps for the right figure. It can be seen that our framework can reduce the total cost considerably.

VII. Conclusions

In this paper, we considered a scenario where a mobile robot is tasked with periodically collecting data from a fixed wireless sensor network. Our goal was to minimize the total cost of the system, including the communication cost of the sensors to the robot, when operating in realistic channel environments, and the motion cost of the robot. We considered a strategy that combines the ideas of clustering and mobile robotic data collection. We then proposed a sub-optimum but computationally-efficient approach to solve this problem by using space-filling curves. More specifically, we showed how the coupled clustering, stop position selection, path planning and motion design problems can be solved as a series of convex optimization problems. We further proposed an iterative fine-tuning strategy inspired by the Lloyd's algorithm. We also mathematically characterized an upper bound for the total energy consumption of our proposed approach, for the case of uniformly-distributed sensors, relating it to key motion and communication parameters. Finally, we verified the effectiveness of our framework in a simulation environment. Our results with realistic channel and motion parameters showed considerable energy saving as compared to the case of no clustering.

References

[1] F. Bullo, E. Frazzoli, M. Pavone, K. Savla, and S. L. Smith. Dynamic vehicle routing for robotic systems. *Proc. of the IEEE*, 2011.

[2] M. M. Zavlanos, M. B. Egerstedt, Y. C. Hu, and G. J. Pappas. Graph-theoretic connectivity control of mobile robot networks. *Proceedings of the IEEE*, 99(9):1525 – 1540, July 2011.

[3] J. Fink, A. Ribeiro, and V. Kumar. Motion planning for robust wireless networking. In *IEEE Int'l Conf. on Robotics and Automation*, 2012.

[4] A. Ghaffarkhah and Y. Mostofi. Communication-aware motion planning in mobile networks. *IEEE Trans. on Automatic Control, special issue on Wireless Sensor and Actuator Networks*, 2011.

This article has been accepted for publication in a future issue of this journal, but has not been fully edited. Content may change prior to final publication. Citation information: DOI 10.1109/TCNS.2016.2574129, IEEE Transactions on Control of Network Systems

[5] A. Ghaffarkhah and Y. Mostofi. Path planning for networked robotic surveillance. *IEEE Trans. on Signal Processing*, 60(7):3560–3575, July 2012.

[6] D. Bhadauria, O. Tekdas, and V. Isler. Robotic data mules for collecting data over sparse sensor fields. *J. of Field Robotics*, 28(3):388–404, 2011.

[7] R. Sugihara and R. Gupta. Improving the data delivery latency in sensor networks with controlled mobility. In *Distributed Computing in Sensor Systems*, pages 386–399. 2008.

[8] R. Sugihara and R. Gupta. Optimal speed control of mobile node for data collection in sensor networks. *IEEE Transactions on Mobile Computing*, 9(1):127–139, 2010.

[9] Y. Yun and Y. Xia. Maximizing the lifetime of wireless sensor networks with mobile sink in delay-tolerant applications. *IEEE Transactions on Mobile Computing*, 9(9):1308–1318, 2010.

[10] J. Luo and J.-P. Hubaux. Joint sink mobility and routing to maximize the lifetime of wireless sensor networks: the case of constrained mobility. *IEEE/ACM Trans. on Networking*, 18(3):871–884, 2010.

[11] W. Heinzelman, A. Chandrakasan, and H. Balakrishnan. An application-specific protocol architecture for wireless microsensor networks. *IEEE Trans. on Wireless Comm.*, 1(4):660–670, 2002.

[12] O. Younis and S. Fahmy. Heed: a hybrid, energy-efficient, distributed clustering approach for ad hoc sensor networks. *IEEE Transactions on Mobile Computing*, 3(4):366–379, 2004.

[13] G. Xing, T. Wang, W. Jia, and M. Li. Rendezvous design algorithms for wireless sensor networks with a mobile base station. In *Proceedings of the 9th ACM international symposium on Mobile ad hoc networking and computing*, pages 231–240, 2008.

[14] O. Jerew, K. Blackmore, and W. Liang. Mobile base station and clustering to maximize network lifetime in wireless sensor networks. *Journal of Electrical and Computer Engineering*, 2012.

[15] M. Ma and Y. Yang. Sencar: an energy-efficient data gathering mechanism for large-scale multihop sensor networks. *IEEE Transactions on Parallel and Distributed Systems*, 18(10):1476–1488, 2007.

[16] A. Somasundara, A. Kansal, D. Jea, D. Estrin, and M. Srivastava. Controllably mobile infrastructure for low energy embedded networks. *IEEE Transactions on Mobile Computing*, 5(8):958–973, 2006.

[17] Y. Yan and Y. Mostofi. Co-optimization of communication and motion planning of a robotic operation under resource constraints and in fading environments. *IEEE Trans. on Wireless Comm.*, 2012.

[18] Y. Yan and Y. Mostofi. To go or not to go: On energy-aware and communication-aware robotic operation. *IEEE Transactions on Control of Network Systems*, 1(3), 2014.

[19] A. Ghaffarkhah and Y. Mostofi. Dynamic coverage of time-varying fading environments. *ACM Trans. on Sensor Networks*, 10(3), April 2014.

[20] A. Ghaffarkhah and Y. Mostofi. Channel learning and communication-aware motion planning in mobile networks. In *Proceeding of IEEE American Control Conference*, pages 5413–5420, Baltimore, MD, July 2010.

[21] Y. Mostofi, M. Malmirchegini, and A. Ghaffarkhah. Estimation of communication signal strength in robotic networks. In *Proc. of the 50th IEEE Int'l Conf. on Robotics and Automation*, May 2010.

[22] M. Malmirchegini and Y. Mostofi. On the spatial predictability of communication channels. *IEEE Trans. on Wireless Comm.*, 2012.

[23] M. Bader. *Space-Filling Curves: An Introduction with Applications in Scientific Computing*, volume 9. Springer, 2012.

[24] Y. Yan and Y. Mostofi. An efficient clustering and path planning strategy in sensor networks for data collection based on space-filling curves. In *IEEE Conference on Decision and Control*, Los Angeles, CA, 2014.

[25] Y. Yan and Y. Mostofi. Efficient communication-aware dynamic coverage using space-filling curves. In *American Control Conference*, Portland, OR, 2013.

[26] J. Bartholdi III and L. Platzman. An $O(N\log N)$ planar travelling salesman heuristic based on spacefilling curves. *Operations Research Letters*, 1(4):121–125, 1982.

[27] J. Bartholdi III and L. Platzman. Heuristics based on spacefilling curves for combinatorial problems in euclidean space. *Management Science*, 34(3):291–305, 1988.

[28] S. Lin and B.W. Kernighan. An effective heuristic algorithm for the traveling-salesman problem. *Operations research*, 21(2):498–516, 1973.

[29] S. Arora. Polynomial time approximation schemes for euclidean traveling salesman and other geometric problems. *J. of the ACM*, 1998.

[30] A. Goldsmith. *Wireless Communications*. Cambridge University Press, 2005.

[31] P. Tokekar, N. Karnad, and V. Isler. Energy-optimal trajectory planning for car-like robots. *Autonomous Robots*, 2013.

[32] R. E. Kirk. *Optimal Control Theory: An Introduction*. Dover Publications, 2004.

[33] C. E. Miller, A. W. Tucker, and R. A. Zemlin. Integer programming formulation of traveling salesman problems. *J. of the ACM*, 1960.

[34] Q. Du, V. Faber, and M. Gunzburger. Centroidal voronoi tessellations: applications and algorithms. *SIAM review*, 41(4):637–676, 1999.

[35] S. Boyd and L. Vandenberghe. *Convex Optimization*. Cambridge University Press, 2004.

[36] W. M. Smith. *Urban Propagation Modeling for Wireless Systems*. PhD thesis, 2004.

Yuan Yan received the BS and MS degrees from Huazhong University of Science and Technology, Wuhan, China, in 2006 and 2008, respectively. He received the PhD degree from the Department of Electrical and Computer Engineering at the University of California Santa Barbara, CA, in 2016. His research interests include robotic router networks and communication-aware motion planning.

Yasamin Mostofi received the BS degree in electrical engineering from Sharif University of Technology, Tehran, Iran, in 1997, and the MS and PhD degrees in the area of wireless communications from Stanford University, California, in 1999 and 2004, respectively. She is currently an associate professor in the Department of Electrical and Computer Engineering at the University of California Santa Barbara. Prior to that, she was a faculty in the Department of Electrical and Computer Engineering at the University of New Mexico from 2006 to 2012. She was a postdoctoral scholar in control and dynamical systems at the California Institute of Technology from 2004 to 2006.

Dr. Mostofi is the recipient of the Presidential Early Career Award for Scientists and Engineers (PECASE), the National Science Foundation (NSF) CAREER award, and IEEE 2012 Outstanding Engineer Award of Region 6. She also received the Bellcore fellow-advisor award from Stanford Center for Telecommunications in 1999 and the 2008-2009 Electrical and Computer Engineering Distinguished Researcher Award from the University of New Mexico. Her research is on mobile sensor networks. Current research thrusts include communication-aware robotics, human-robot networks, RF sensing, X-ray vision for robots, see-through imaging, and occupancy estimation. Her research has appeared in several reputable news outlets such as BBC, Huffington Post, Daily Mail, Engadget, and NSF Science360. She has served on the IEEE Control Systems Society conference editorial board 2008-2013. She is currently an associate editor for the IEEE TRANSACTIONS ON CONTROL OF NETWORK SYSTEMS. She is a senior member of the IEEE.